2020 IMEKO TC-4 International Conference on
Metrology for Archaeology and Cultural Heritage
Trento, Italy, October 22-24, 2020

Point clouds registration based on constant radius features for large and detailed cultural heritage objects

Di Angelo L.[1], Di Stefano P.[1], Morabito A.E.[2], Guardiani E.[1]

[1] *Department of Industrial and Information Engineering, and of Economics – University of L'Aquila, via G. Gronchi 18 L'Aquila, Italy, {luca.diangelo,paolo.distefano,emanuele.guardiani}@univaq.it*

[2] *Department of Engineering for Innovation – University of Salento, via per Monteroni, Lecce, Italy, annaeva.morabito@unisalento.it*

Abstract – **The registration permits to positioning in a single reference system point clouds acquired from different points of view. Since this is typically obtained with an iterative numerical method, it represents an important source of error in the entire reverse engineering process. As all iterative methods, such errors depend on the choice of the initial solution; therefore, this process requires an expert user who, by using dedicated software, choices the sequence of clouds to be registered, imposes for each pairwise the first attempt registration, launches the iterative method, and verifies the final result. With the aim to minimize the error and the user's interaction, some devices are proposed in the market (turntable or the anthropomorphic arm, etc.). The above-mentioned hardware and software tools cannot be used in the cultural heritage applications involving large and detailed objects. In this paper, an automatic alignment method of point clouds is proposed. The method uses as inputs the constant radius features, which are frequently detectable on cultural heritage objects. The automatic alignment of the point clouds is based on the recognition, the segmentation, and the registration of the sweep lines identifiable from these features.**

I. INTRODUCTION

Registration of point clouds captured by 3D scanners is of fundamental importance to many areas of research, such as computer vision ([1] and [2]), computer graphics [3], robotics ([4] and [5]) and geometric inspection. The aim is to compute the geometric transformation that optimally aligns pairs of point sets so that multiple datasets are merged into a common coordinate system. This is a challenging task, due to the following difficulties: unknown relative positions of the input data, noisy input data, variable point density of the point clouds and partial overlap between two data sets.

In the 3D reconstruction of cultural heritage, point set registration is an important prerequisite for complete geometric model reconstruction. Due to the occlusion, in fact, an object cannot be entirely scanned from a single viewpoint. Therefore, the 3D scanner has to acquire point sets from different viewpoints to cover the entire surface of the object. These point sets, then, must be transformed into one common reference frame for 3D model reconstruction. Such a transformation can be achieved with multi-view registration of point sets acquired from different viewpoints. According to the number of point sets involved, the registration problem can be roughly divided into pair-wise registration and multi-view registration, with the former addressed relatively extensively. Point set registration can be used also to automatically search the matching between fragments of the same object. In this case, the alignment of fracture surfaces must be searched.

The Iterative Closest Point (ICP) is one of the most used algorithms for aligning 3D point clouds. From an initial alignment, an iterative process minimizes the distances between the point clouds. In this algorithm, first introduced by Chen and Medioni [6] and Besl and McKay [7], one-point cloud (the reference or the target) is kept fixed and the other (the source) is transformed to best match the reference. The rigid-body transformation, which is a combination of translation and rotation, is iteratively refined to minimize an error metric, usually described by the sum of the differences squared between the coordinates of the matched pairs. The ICP algorithm has low computational complexity and can support parallel computing devices. However, the ICP algorithm demands an accurate initial guess and requires the closest point pairs are determined.

In [8] Rusinkiewicz et al. identify six parts of the ICP algorithm that researchers have been improving over the years: point selection, neighborhood selection, point matching, weighting pairs, outlier rejection, and error minimization.

In addition to the coordinates of the points, the alignment of 3D point clouds can be carried out by extracting some 3D local descriptors. These descriptors usually calculate the statistics of local geometric properties, such as surface normals and curvatures. A comprehensive review of 3D point cloud descriptors can be found in [9]. These descriptors often suffer from low descriptiveness, since they cannot provide a comprehensive and unambiguous representation of local shape geometry. These geometric properties are affected by uncertainties due to the quality and resolution of point clouds, surface noise, and single outliers.

Point set registration is also used in industrial geometric inspection processes for aligning the 3D point cloud of the measured object with its CAD model so that they can be compared and the relative differences measured. In this case, the point cloud/CAD model alignment is generally driven by a geometric feature-based approach. An analytical geometric feature of the CAD model is aligned with the corresponding recognized geometric feature in the point cloud. Analytical features, however, do not generally characterize the artefacts of Cultural Heritage, nor fractured surfaces are simple geometries such as plane, cylinder, or cone.

Since the registration of point clouds is typically obtained with an iterative numerical method, it represents an important source of error in the entire reverse engineering process. As all iterative methods, such errors depend on the choice of the initial solution. This process requires, therefore, an expert user who, by using dedicated software, choices the sequence of clouds to be registered, imposes for each pairwise the first attempt registration, launches the iterative method, and verifies the result. With the aim to minimize the error and the user's interaction, some devices have been proposed in the market (such as turntable or anthropomorphic arm).

The hardware and software tools mentioned above, however, exhibit several problems when used in cultural heritage applications involving large and detailed objects. For this reason, this paper

II. THE POINT CLOUDS REGISTRATION METHOD

The alignment method of point clouds, which is based on a feature recognition process, is sketched in the flowchart of Figure 1. The method takes advantage of the capability to recognize non-conventional geometric features such as the constant radius features [10].

III. CONSTANT RADIUS FEATURE DESCRIPTOR

A constant radius feature $\varphi_{ij}(r_i)$ is a portion of the object surface, which develops along a trajectory (called *sweep line*) whose principal section is quite circular. The characteristic radius r_i of this section is almost constant along the feature. In the cultural heritage these features occur frequently. For example, these features are usually detectable in some anatomic details of the human body. In Figure 2a) the points belonging to several features φ_{ij} with $r_i \approx 5.5$ mm are evidenced. These features have been recognized automatically from the bust extracted by the tessellated model of the Neptune with Trident of Bologna by using a methodology recently developed [10].

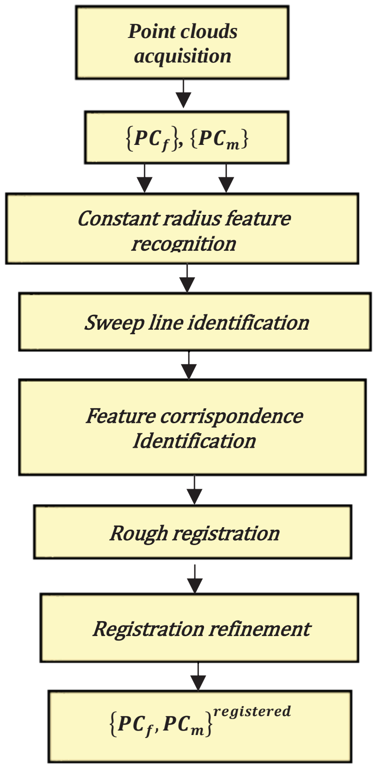

Fig. 1. Flow-chart of the methodology

A. Constant radius feature recognition

The proposed methodology consists of the following three steps:

- estimation of the differential geometrical properties (normal and curvatures) at each node of the tessellated model;
- evaluation of the characteristic radii r_i of the constant radius features $\varphi_{ij}(r_i)$ of the object;
- segmentation of the features $\varphi_{ij}(r_i)$ for each r_i-value.

Based on the results reported in [14], in this paper the differential geometrical properties are evaluated at each node by using methods robust with respect to noise: the *medial quadric method* for the normal versor and the *5-coefficients paraboloid fitting method* for the principal curvatures.

In order to evaluate preliminarily the characteristic radii r_i, an analysis of the occurrences of the r-values at the mesh nodes is carried out where the r_i-values are estimated from the histogram's peaks. However, due to the uncertainties affecting the r-values (as also shown by the color map shown in Figure 2b), the peaks of the histogram are often not well defined (see as example the histogram in Figure 3 for the bust reported in Figure 2). In particular, a peak blur effect, growing with the r-values, is usually observed which can be so relevant to cover other potentially useful peaks. In other cases, some fictitious peaks unrelated to real features may appear [13]. To cope with this lack of well-defined peaks an iterative methodology was implemented: at the end of the *i-th* iteration, the points recognized as belonging to the features $\varphi_{ij}(r_i)$ with r_i equal to the peak value of the histogram are removed from the evaluation of r-histogram of the subsequent iteration *i+1-th*. This iterative process is repeated until there are no more significant peaks in the histogram.

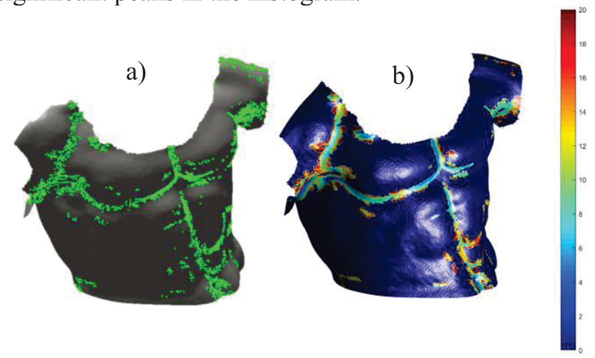

Fig. 2. Points recognized as belonging to several features $\varphi_{ij}(r_i)$ with r_i≈5.5 mm (a). Color map of the minimum curvature radius r (b).

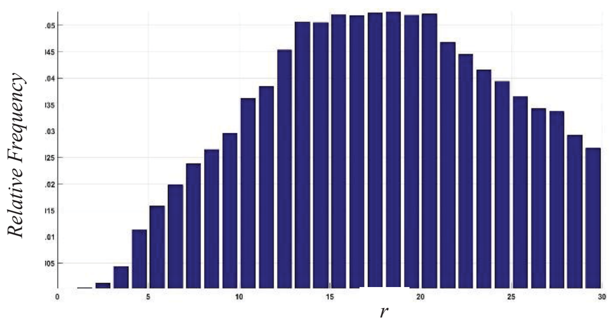

Fig. 3. Histogram of the r-values for the bust of Figure 1

The nodes belonging to a feature $\varphi_{ij}(r_i)$ are characterized by values of the minimum curvature radius r usually affected by significant uncertainty, as shown by the color map of radii shown in Figure 2b). This variability is due to several factors (as described in detail in [12]) and makes the detection of these features a not trivial process. In order to deal with this variability, a fuzzy approach was developed for the automatic recognition of the features $\varphi_{ij}(r_i)$. The fuzzy approach classifies unequivocally the points of the tessellated model according to three following categories:

- points belonging to feature $\varphi_{ij}(r_i)$;
- points belonging to sharp edges;
- generic (or residual) points.

The segmentation of the tessellated model according to these categories requires the definition of three membership functions, denoted respectively by μ_i, μ_E and μ_G. Each of them measures the possibility that the generic node **p** of the object mesh belongs to one of the aforementioned categories. Since **p** can belong unequivocally only to those three categories, these functions must always satisfy the following equation:

$$\mu_i + \mu_E + \mu_G = 1 \qquad (1)$$

To establish the membership of the generic point to one of the afore-mentioned categories, some node properties, able to affect this membership attribution, have to be considered. For the membership function μ_E, the property considered is the sharpness indicator (*SHI*), which compares the normal vector evaluated at the generic point **p** by a smooth function approximating the *h-ring neighborhood* with the normals to each planar facet belonging to **p** neighborhood. To describe analytically the membership function μ_E a ramp function was selected (Figure 4a).

The node property considered for μ_i evaluation is the quality of the surface tessellation, which can be measured by the factor of curvature approximation γ. This factor, defined as "the maximum value of the tangent of the dihedral angles between adjacent triangular facets incident at **p**", measures how well the geometry of a regular curved surface is described by the discrete model. A well-sampled surface is characterized by very small γ values. In particular, γ is 0 at each point of a flat surface independently from the quality of tessellation. For curved surfaces, γ increases as the surface is more coarsely sampled. For μ_i evaluation, a trapezoidal function was selected (Figure 4b). In the figure σ and t are experimental parameters estimated to take into account of the r-variability due to the handmade manufacturing of the cultural heritage.

In Figure 5, the color map of the membership function μ_i highlights the nodes for which a non-zero possibility of attribution to the features φ_{ij} is identified.

These color maps, however, do not allow distinguishing the single features φ_{ij} from each other and from the other features. For this purpose, a further and last step, called *region growing*, is required [14]. The *region growing* starts from a *seed node* of the mesh selected among the nodes where the maximum membership degree μ_i is reached. The seed node is compared with every node $\mathbf{p}_j$ belonging to the 1-ring neighborhood to analyze the similarity. The nodes recognized as similar are aggregated in the growing region. The growing algorithm stops when dissimilar nodes are met or all the mesh nodes have been analyzed.

Figure 6 shows the nine *constant radius features* $\varphi_{ij}(r_i)$ with r_i≈5.5 mm recognized on the bust of Figure 1.

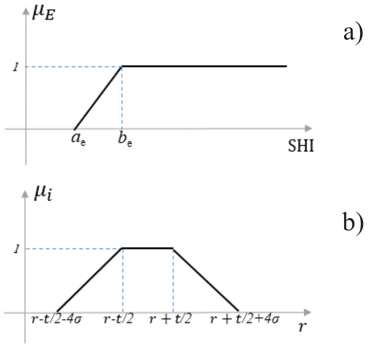

Fig. 4. The ramp function for μ_E (a). The trapezoidal function for μ_i.

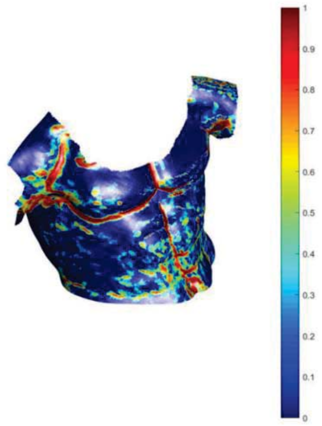

Fig. 5. Color map of the membership function μ_i for the bust of Figure 1

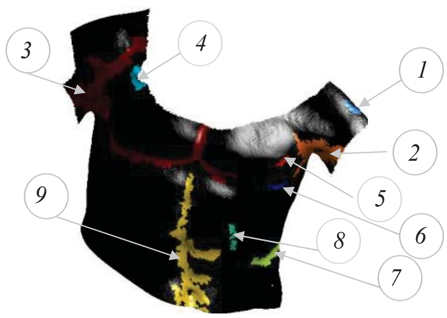

Fig. 6. The nine constant radius features $\varphi_{ij}(r_i)$ with r_i≈5.5 mm recognized on the bust of Figure 1.

B. How to identify the feature sweep line

For each recognized constant radius feature, the sweep line is identified by its voxelization. The features $\varphi_{ij}(r_i)$ described by voxels are processed so that their sweep lines are evaluated by using the methodology described in [15]. The sweep line $CRFD_j$ of the j-th feature $\varphi_{ij}(r_i)$ is defined by the set of points $\wp_j$ located on the sweep line. Figures 7 a) and b) show respectively the 8-th *constant radius feature* $\varphi_{ij}(r_i \approx 5.5)$ recognized on the bust of Figure 5 and the corresponding *CRFD.*

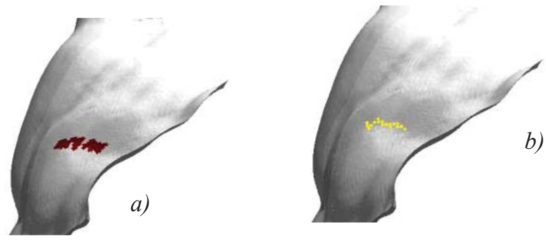

Fig. 7. The 8-th CRFD for the feature $\varphi_{ij}(r_i \approx 5.5)$ recognized on the bust of Figure 5

At the end of this step, the two point clouds to be registered are segmented in terms of *CRFD*. PC_f and PC_m are the sets of CRFD, pertaining respectively to the fixed and to the moving point clouds and identified for different values of the characteristic radius r_i.

IV. COARSE-TO-FINE POINT CLOUD REGISTRATION ALGORITHM

The aim of the 3D point cloud registration is to find the rotation matrix **R** and the translation vector **t** for which:

$$\sum_{min}\left\|\boldsymbol{R}\cdot PC_m + \boldsymbol{t} - PC_f\right\| \quad (2)$$

where PC_f and PC_m are, respectively, the fixed and moving point clouds.

At this purpose, the proposed method consists of three steps: correspondences generation, coarse registration and fine registration.

A. Feature Correspondence Identification

The search of the correspondences between the point clouds PC_f and PC_m is an essential task for a suitable registration.

In the proposed method, the correspondence generation is performed by taking into account all the possible combinations among the sweep lines $CRFD_j^{f,r_i}$ of the features $\varphi_{ij}(r_i)$, recognized for a given value of the characteristic radius r_i from the fixed point cloud PC_f and the sweep lines $CRFD_h^{m,r_i}$ detected from the features $\varphi_{ij}(r_i)$ of the moving cloud PC_m for the same radius r_i.

For each configuration, the first attempt solution is obtained by aligning the convolution matrix eigenvectors of the points belonging to $CRFD_h^{m,r_i}$ to those ones of $CRFD_j^{f,r_i}$.

The ICP method is applied point-to-point to obtain a more accurate configuration. Being $\wp_{\{CRFD_h^{m,r_i}\}}$ and $\wp_{\{CRFD_j^{f,r_i}\}}$, respectively, the coordinates of the points $CRFD_h^{m,r_i}$ and $CRFD_j^{f,r_i}$ and τ_d a threshold value, $CRFD_h^{m,r_i}$ and $CRFD_j^{f,r_i}$ are considerated as candidates for a correspondence if the following inequality is verified:

$$\sum_{\boldsymbol{mean}} \left\| \boldsymbol{R} \cdot \wp_{\left\{CRFD_h^{m,r_i}\right\}} + \boldsymbol{t} - \wp_{\left\{CRFD_j^{f,r_i}\right\}} \right\| < \tau_d \qquad (3)$$

By aligning the convolution matrix eigenvectors based on the correspondences found with the afore-mentioned methodology, a rough registration between the point clouds PC_f and PC_m can be performed.

B. Registration refinement

Fine registration is performed by an ICP algorithm, minimizing the following function specifically designed:

$$\frac{\sum_{j=1}^{n} w_j d\left(\boldsymbol{p_j}, TS(PC_f)\right)}{\sum_{j=1}^{n} w_j} \qquad (4)$$

where:

- n is the number of points of PC_m;
- $\boldsymbol{p}_j$ is the j – th point belonging to PC_m;
- $TS(PC_f)$ is the tessellated surface relative to the fixed point cloud PC_f;
- $d(\boldsymbol{p}_j, TS(PC_f))$ is the distance between $\mathbf{p}_j$ and the tessellated surface $TS(PC_f)$ according to the following equation:

$$d\left(\boldsymbol{p_j}, TS\left(PC_f\right)\right) = \min_{\boldsymbol{q_{i,j}} \in TS(PC_f)} \left\|\boldsymbol{q_{i,j}} - \boldsymbol{p_j}\right\|_2 \qquad (5)$$

where $q_{i,j}$ is a point belonging to the target point cloud PC_m.

- $w_i = \max(\mu_i, 0.5)$ is a weight, which gives more importance to those points characterized by high values of the membership function μ_i for a given characteristic radius r_i.

Figure 8 shows how to evaluate $\boldsymbol{q}_{i,j}$ and the distance d in the 2D case.

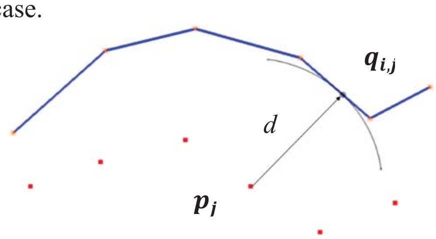

Fig. 8. How to evaluate the point $\boldsymbol{q}_{i,j}$ and the distance d in 2D.

The weights w_i play an important role for the functionalities of the method presented here and they are evaluated based on the membership function μ_i. This function, measuring the possibility that the generic node **p** of the object mesh belongs to a feature $\varphi_{ij}(r_i)$, is, therefore, very important into the approach proposed here for the registration of point clouds.

V. RESULTS

In order to quantify the performance of the proposed method, henceforth labelled as the *CRFD*-based method, the real test case of figure 9 has been chosen: it is a garden dwarf whose geometry is critical for methods based on the search for individual point correspondences. The model has been scanned by a 3D laser scanner (FARO Edge, 9 ft (2.7 m)), where the single point repeatability was less than 0.064 mm. The average point spacing of the point cloud was set to 0.15 mm. Each of the acquired point clouds has been processed for generating a valid triangular mesh by using a commercial software (Geomagic®).

With the aim to apply the proposed method, two different points cloud are considered in figure 10: the fixed point cloud PC_f (figure 10a) and the moving point cloud PC_m (figure 10b). In figure 11, the features $CRFD$ identified for three characteristic radii from the two points clouds of figure 10, are shown.

Fig. 9. The test case considered here

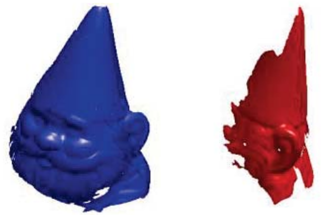

a) PC_f *b) PC_m*

Fig. 10. The two points clouds of the test case considered here

In order to remove the possible false positives from the *CRFD*-correspondences, a dimensional analysis is performed. Figure 12 shows the results of this analysis by aligning the correspondences with a threshold value τ_d of 0.75mm.

In figure 13, the final configuration distance map for the first attempt configuration of figure 12 is depicted.

With the aim to quantify the performances of the proposed method, the same points clouds are registered by using the commercial software Geomagic®. The applied tool is, in particular, the *Manual Registration*: after the user selected the corresponding points on the two points clouds, the software minimizes their distances by an iterative method. Figure 14 compares the normalized histograms of the distances point-triangles obtained for the two final aligned configurations. At present, the fully automatic method proposed here achieves similar performances.

VI. CONCLUSIONS

In this paper, an automatic alignment method of two points clouds experimentally acquired is proposed. The method uses as inputs the constant radius features $\varphi_{ij}(r_i)$, which are frequently detectable on the artefacts of cultural heritage. These features can be automatically recognized from the tessellated models by a fuzzy methodology previously developed by the authors. The approach proposed for the automatic alignment of the point clouds performs the recognition, the segmentation, and the registration of the sweep lines identifiable from the features $\varphi_{ij}(r_i)$. The main limit of the method is that it correctly finds the correspondences in the case that the same feature is almost entirely present in the two points clouds to be registered. Future efforts should aim at verifying and improving the method in terms of time consumption, robustness to small overlaps, mesh resolution and points irregularity.

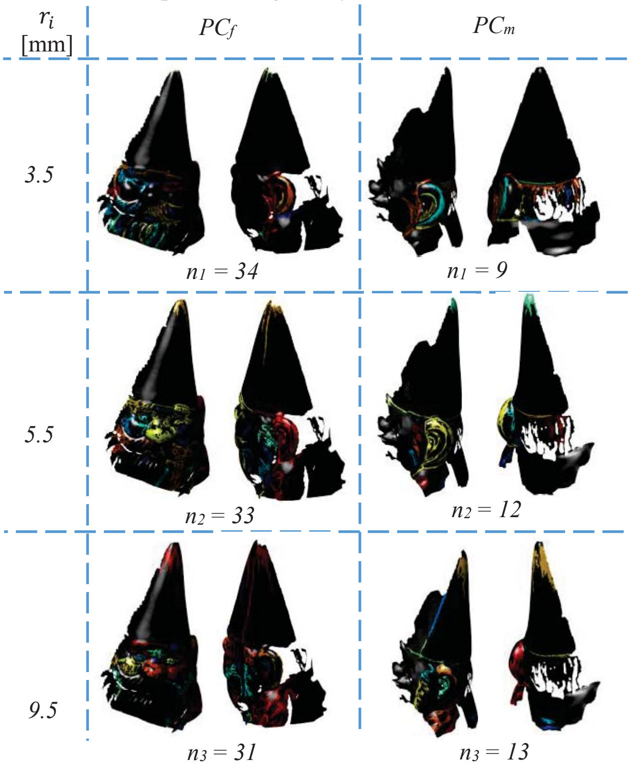

Fig. 11. The CRFDs identified for the point clouds of figure 10

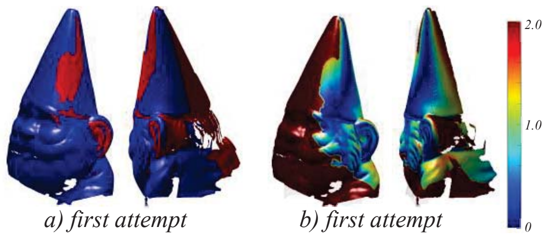

a) first attempt configuration *b) first attempt configuration distance map*

Fig. 12. First attempt configuration (a) and distance map (b) for the point clouds of figure 7

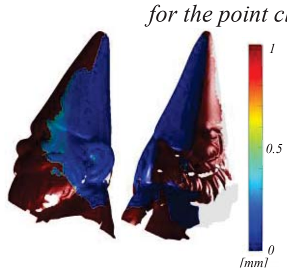

Fig. 13. Final configuration distance map for the point clouds of figure 7

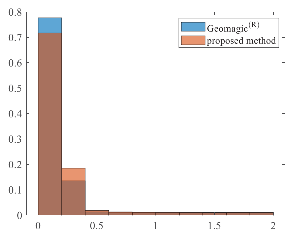

Fig. 14. Comparison of the normalized histograms of distances point-triangles

REFERENCES

[1] L. Li, M. Yang, C. Wang , B. Wang, “Robust point set registration using signature quadratic form distance”, IEEE Trans. Cybern. (2018) 1–13.

[2] J. Yang, H. Li, D. Campbell, Y. Jia, “Go-ICP: a globally optimal solution to 3D ICP point-set registration”, IEEE Trans. Pattern Anal. Mach. Intell. 38 (11) (2016) 2241–2254.

[3] A. Dai, M. Nießner, M. Zollhöfer, S. Izadi, C. Theobalt, “Bundlefusion: Real-time globally consistent 3D reconstruction using on-the-fly surface reintegration”, ACM Trans. Graphics (TOG) 36 (3) (2017) 24 .

[4] L. Ma, J. Zhu, L. Zhu, S. Du, J. Cui, “Merging grid maps of different resolutions by scaling registration”, Robotica 34 (11) (2016) 2516–2531 .

[5] F. Yu, J. Xiao, T. Funkhouser, “Semantic alignment of lidar data at city scale”, in: IEEE Conference on Computer Vision and Pattern Recognition (CVPR).

[6] C. Yang, G. Medioni (1991). "Object modelling by registration of multiple range images". Image Vision Comput. 10 (3): 145–155.

[7] P. J. Besl, N.D. McKay (1992). "A Method for Registration of 3-D Shapes". IEEE Transactions on Pattern Analysis and Machine Intelligence. 14 (2): 239–256. doi:10.1109/34.121791.

[8] S. Rusinkiewicz, M. Levoy, “Efficient variants of the ICP algorithm”, in: Proceedings of the Third International Conference on 3-D Digital Imaging and Modeling, IEEE, 2001, pp. 145–152.

[9] X.F. Hana, J.S. Jin, J. Xie, M.J. Wang, W. Jiang, “A comprehensive review of 3D point cloud descriptors”, ArXiv, 2018, abs/1802.02297.

[10] L. Di Angelo, P. Di Stefano, A.E. Morabito, C. Pane, (2018). “Measurement of constant radius geometric features in archaeological pottery”. Measurement: Journal of the International Measurement Confederation, 124, 138-146.

[11] L. Di Angelo, P. Di Stefano, “Experimental comparison of methods for differential geometric properties evaluation in triangular meshes”, Comput. Design Appl. 8(2) (2011) 193–210.

[12] L. Di Angelo, P. Di Stefano, A.E. Morabito (2018). “Secondary features segmentation from high-density tessellated surfaces”. International Journal on Interactive Design and Manufacturing, 12(3), 801-809.

[13] L. Di Angelo, P. Di Stefano, A.E. Morabito (2017). “Segmentation of secondary features from high-density acquired surfaces”. (2017) Lecture Notes in Mechanical Engineering, pp. 1043-1051..

[14] L. Di Angelo, P. Di Stefano, A.E. Morabito, C. Pane, (2019). “Constant radius geometric features segmentation in archeological pottery”. IMEKO International Conference on Metrology for Archaeology and Cultural Heritage, MetroArchaeo 2017, 69-74.

[15] Y. Zhou, A.W. Toga (1999). “Efficient skeletonization of volumetric objects”. IEEE Transactions on visualization and computer graphics, 5(3), 196-209.